HHS Public Access

Author manuscript

J Control Release. Author manuscript; available in PMC 2019 November 10.

Published in final edited form as:

J Control Release. 2018 November 10; 289: 114–124. doi:10.1016/j.jconrel.2018.09.020.

Investigation of Tunable Acetalated Dextran Microparticle Platform to Optimize M2e-Based Influenza Vaccine Efficacy

Naihan Chen[#a], **Matthew D. Gallovic**[#a], **Pamela Tiet**[a], **Jenny P.-Y. Ting**[b,c,d,e], **Kristy M. Ainslie**[a,c], and **Eric M. Bachelder**[a,*]

[a] Division of Pharmacoengineering and Molecular Pharmaceutics, Eshelman School of Pharmacy, University of North Carolina, Chapel Hill, NC, USA

[b] Department of Genetics, Lineberger Comprehensive Cancer Center, University of North Carolina, Chapel Hill, NC, USA

[c] Department of Microbiology and Immunology, University of North Carolina, Chapel Hill, NC, USA

[d] Institute for Inflammatory Diseases, University of North Carolina, Chapel Hill, NC, USA

[e] Center for Translational Immunology, University of North Carolina, Chapel Hill, NC, USA

[#] These authors contributed equally to this work.

Abstract

Influenza places a significant health and economic burden on society. Efficacy of seasonal influenza vaccines can be suboptimal due to poor matching between vaccine and circulating viral strains. An influenza vaccine that is broadly protective against multiple virus strains would significantly improve vaccine efficacy. The highly conserved ectodomain of matrix protein 2 (M2e) and 3′3′ cyclic GMP-AMP (cGAMP) were selected as the antigen and adjuvant, respectively, to develop the basis for a potential universal influenza vaccine. The magnitude and kinetics of adaptive immune responses can have great impact on vaccine efficacy. M2e and cGAMP were therefore formulated within acetalated dextran (Ace-DEX) microparticles (MPs) of varying degradation profiles to examine the effect of differential vaccine delivery on humoral, cellular, and protective immunity. All Ace-DEX MP vaccines containing M2e and cGAMP elicited potent humoral and cellular responses *in vivo* and offered substantial protection against a lethal influenza challenge, suggesting significant vaccine efficacy. Serum antibodies from Ace-

[*]**Corresponding Author**, Eric M. Bachelder, Research Assistant Professor, UNC Eshelman School of Pharmacy, Division of Pharmacoengineering and Molecular Pharmaceutics, 4210 Marsico Hall, 125 Mason Farm Road, Chapel Hill, NC 27599, ebacheld@email.unc.edu.

Conflict of Interest

Drs. Ainslie, Bachelder, and Ting serve on the advisory board for IMMvention Therapeutix, Inc. Although a financial conflict of interest was identified for management based on the overall scope of the project and its potential benefit to IMMvention Therapeutix, Inc., the research findings included in this publication may not necessarily be related to the interests of IMMvention Therapeutix, Inc. The terms of this arrangement have been reviewed and approved by the University of North Carolina at Chapel Hill in accordance with its policy on objectivity in research.

DEX MP vaccinated mice also demonstrated cross reactivity against M2e sequences of various viral strains, which indicates the potential for broadly protective immunity. Of all the formulations tested, the slowest-degrading M2e or cGAMP MPs elicited the greatest antibody production, cellular response, and protection against a viral challenge. This indicated the importance of flexible control over antigen and adjuvant delivery. Overall, robust immune responses, cross reactivity against multiple viral strains, and tunable delivery profiles make the Ace-DEX MP platform a powerful subunit vaccine delivery system.

Keywords

influenza vaccine; tunable delivery; cGAMP adjuvant; microparticle; cross protection; immune activation

1. Introduction

Influenza poses considerable impact worldwide, both on community health and the economy. The Centers for Disease Control and Prevention estimate that between 9.2 and 35.6 million people become infected with the flu in the United States each year, with up to 710,000 hospitalizations and 56,000 flu-associated deaths [1]. Annual influenza outbreaks also cause substantial economic burden totaling more than $87 billion from direct medical costs and projected loss of earnings [2]. Vaccination represents the most effective public health measure at preventing influenza infection. However, the effectiveness of seasonal influenza vaccines varies widely from season to season and can be as low as 10%, as was experienced in 2004 [3]. Low efficacy can be contributed to three major factors that lead to mismatched vaccine and circulating viral strains: (1) inadequate predictions, (2) viral drift and shift, and (3) egg-adapted antigenic changes that occur during chicken egg-based vaccine production [4]. Therefore, vaccines that elicit more broad immunity against multiple influenza virus strains and circumvent the shortcomings of egg-based production are needed.

An option for fulfilling these needs is developing vaccines that include more conserved influenza viral epitopes. One of these, the ectodomain of matrix protein 2 (M2e), is essential for viral replication and highly conserved across different influenza A viruses [5]. Although M2e has been explored in pre-clinical and early phase clinical trials as a vaccine antigen, it is poorly immunogenic and typically requires co-delivery of a vaccine adjuvant [4]. Aluminum salts (alum), squalene-based oil-in-water emulsions (MF59 or AS03), AS04 (3-O-desacyl-4’-monophosphoryl lipid A (MPL) adsorbed to alum), $AS01_B$ (liposomal MPL and the saponin QS-21), and CpG 1018 are currently the only FDA-approved adjuvants [6–8]. Each of them has significant drawbacks. For instance, alum, MF59, and AS03 all induce Th2-biased humoral immunity, and are unable to induce significant cellular immunity required for many intracellular pathogens such as influenza [9]. AS04 includes many of the drawbacks of alum and does not offer controlled delivery of MPL. The vaccine formulation containing CpG 1018 requires 3 mg of the agonist, which is highly impractical for broad application. Given the drawbacks of these adjuvants, including their limited ability to provide a balance of humoral and cellular immunity, alternative ones are needed. The family of cyclic dinucleotides (CDNs) are an attractive option because they have potent

immunostimulatory properties and the ability to induce strong humoral and cellular responses [10, 11]. Due to these advantageous properties, soluble CDNs have previously been used in several seasonal flu vaccine formulations [12–18]. Since the cytosolic location of STING (stimulator of interferon genes) limits the accessibility of its charged CDN agonists, several groups, including us, have designed CDN-loaded drug delivery systems to enable more efficient delivery in various biological models [11, 19–25].

The system we used is based on the biopolymer acetalated dextran (Ace-DEX). Via a one-step reaction, Ace-DEX can be synthesized from FDA-approved dextran [26–28]. When formulated into drug delivery systems, Ace-DEX microparticles (MPs) are acid-sensitive, stable under elevated temperatures, and can passively target antigen-presenting cells (APCs) based on particle size [29, 30], making them advantageous for subunit vaccines and other immunomodulatory applications [11, 31, 32]. Moreover, Ace-DEX MPs have tunable degradation rates, which provide them with unique advantages compared to other delivery platforms. Based on the polymer synthesis reaction time, varying degrees of cyclic or acyclic acetal group coverage (i.e., relative cyclic acetal coverage, CAC) can be achieved [33]. By controlling MP CAC or polymer molecular weight, degradation half-lives can range from hours to months. Despite some flexibility in degradation kinetics of delivery vehicles formulated using other acid-sensitive polymers, such as poly(β-amino) esters (PBAEs), poly(ortho esters) (POEs), or polyketals, modulating degradation half-lives is achieved mostly through less straightforward chemical modifications or using polymer blends [34–36].

Considering the distinct timelines of processes and signaling pathways that are involved between vaccine administration and development of protective immunity (e.g., trafficking/distribution of vaccine components, antigen processing, generation of memory response), kinetics of antigen and adjuvant delivery can have a substantial impact on immune activation and vaccine outcomes [37–41]. Conventional delivery methods (e.g., alum) that slowly release antigen and adjuvant with little control over their delivery kinetics may be suboptimal [42, 43]. Ace-DEX MPs, on the other hand, enable flexible, precise control over antigen and adjuvant delivery, and can provide a tool to examine *in vitro* and *in vivo* immune activation kinetics, as well as optimize peak and duration of humoral and cellular immunity.

We have previously demonstrated that antigen-loaded Ace-DEX MPs of lower CAC resulted in higher antigen cross-presentation [27], and adjuvant-loaded Ace-DEX MPs with certain CACs achieved greater immunostimulation [44]. When using MPs of varying CACs in a model vaccine composed of the antigen ovalbumin (OVA) and adjuvant nucleotidebinding oligomerization domain-containing protein 2 (NOD2) agonist murabutide, we have demonstrated controlled humoral and cellular immune responses [45].

Because Ace-DEX MP degradation half-life appears to have an effect on humoral and cellular responses, this study aims to identify the optimal degradation rate of M2e (antigen)- and CDN 3’3’-cGAMP (adjuvant)-loaded Ace-DEX MPs. Release kinetics of cGAMP from Ace-DEX MPs with varying CACs were characterized under both neutral (pH 7.4) and acidic (pH 5.0) conditions. To evaluate the effect of controlled antigen or adjuvant delivery on immune activation kinetics, we vaccinated mice with M2e or cGAMP MPs of different

CACs and examined the magnitude and kinetics of humoral and cellular responses *in vivo* over a 10-week period. Protective efficacy of Ace-DEX MP vaccines was evaluated through a lethal influenza viral challenge. Finally, the potential for cross-reactivity against multiple flu strains was determined through endpoint antibody titers against M2e sequences of different viral origins.

2. Materials and Methods

2.1. Materials

The M2e consensus peptide (SLLTEVETPIRNEWGCRCNDSSD, isoelectric point pH 3.95), the A/Puerto Rico/8/34 and A/Victoria/3/75 M2e sequence (SLLTEVETPIRNEWGCRCNGSSD, isoelectric point pH 4.15) [46, 47], the A/Hebei/19/95 M2e sequence (SLLTEVETPIRNEWECRCNGSSD, isoelectric point pH 3.99) [46], and the A/Thailand/SP-83/04 and A/Vietnam/1203/2004 M2e sequence (SLLTEVETPTRNEWECRCSDSSD, isoelectric point pH 3.84) [47, 48] were synthesized by CS Bio (Menlo Park, CA). Underlined amino acids indicate differences from the consensus sequence. Peptide isoelectric points were determined using GenScript's Peptide Property Calculator [49]. 3'3'-cGAMP (cGAMP) and the MF59-like squalene oil-in-water emulsion vaccine adjuvant AddaVax was purchased from InvivoGen (San Diego, CA). Purified influenza virus A/Puerto Rico/8/1934 (PR8; Charles River) was diluted in ultra-pure PBS, aliquotted, and stored at −80°C to generate mouse infection stocks. All other reagents were purchased from Sigma-Aldrich (St. Louis, MO) and used unmodified unless otherwise noted. In the presence of Ace-DEX polymer or MPs, basic water (pH 9.0) containing 0.04% v/v triethylamine (TEA) was used to minimize polymer degradation.

2.2. Synthesis and characterization of acetalated dextran

Ace-DEX was synthesized and characterized following previously published literature [33]. To obtain 'low,' 'medium,' and 'high' CAC, dextran (from *Leuconostoc mesenteroides*, average molecular weight of 70 kDa) was reacted with 2-ethoxypropene (Matrix Scientific, Elgin, SC) for 3, 22, or 1,440 min. Polymer CAC was determined to be 'low' (18–20%), 'medium' (39–42%), or 'high' (60–62%) using ^{1}H nuclear magnetic resonance (NMR) spectroscopy. These polymers will be referred to as Ace-DEX (20%), Ace-DEX (40%), or Ace-DEX (60%) in the manuscript for simplicity.

2.3. Formulation of blank, M2e-, or cGAMP-loaded microparticles

Ace-DEX MPs were fabricated using a double-emulsion water/oil/water (w/o/w) solvent evaporation method [32]. Ace-DEX polymers of varying CAC (200 mg) were dissolved in ethyl acetate (2 mL) and mixed with PBS (400 μL) containing M2e (the M2e consensus peptide SLLTEVETPIRNEWGCRCNDSSD) and/or cGAMP (1 mg). This mixture was homogenized for 30 sec at 21,000 RPM (IKA T25 Digital Ultra-Turrax, Cole Parmer, Vernon Hills, IL), 12 mL poly(vinyl alcohol) (3%, PVA) was added, and the mixture was homogenized for another 30 sec. The emulsion was stirred for 3 hours in 0.3% PVA, before the particles were collected via centrifugation at 24,000 × g at 4 °C for 10 min (Thermo Scientific Sorvall Legend XTR centrifuge, Waltham, MA). The pellet was washed twice with basic water, and then frozen and lyophilized for 2 days prior to analysis. Blank MPs

were prepared following the same procedure using Ace-DEX (40%) without the addition of any antigen or adjuvant. All Ace-DEX MPs were prepared using methods to keep endotoxin levels low, these methods included using freshly prepared solutions and clean glassware that was soaked in 1.0 M sodium hydroxide prior to use.

2.4. Physical characterization of Ace-DEX MPs

The diameter and polydispersity index of Ace-DEX MPs were measured by dynamic light scattering (Brookhaven NanoBrook 90Plus Zeta Particle Size Analyzer, Holtsville, NY) and reported as mean diameter by number [33]. MP zeta potential was measured using the same instrument. Scanning electron microscopy (SEM) images were also obtained to examine the size and morphology of these MPs using an S-4700 Cold Cathode Field Emission Scanning Electron Microscope (Hitachi High-Technologies, Krefeld, Germany). Endotoxin content of all MP sets was assessed using the Pierce LAL Chromogenic Endotoxin Quantitation Kit following the manufacturer's protocol (Thermo Scientific, Waltham, MA). All endotoxin levels were undetectable (< 0.125 EU/mg), well within the limits of many preclinical formulations [50].

2.5. Quantification of Encapsulated M2e and cGAMP

Encapsulation efficiencies of M2e and cGAMP were measured using high performance liquid chromatography (HPLC) (Agilent 1100 series HPLC, Santa Clara, California). MPs were dissolved in triplicate in water:acetonitrile (75:25, v/v) with 0.1% v/v trifluoroacetic acid (TFA). The mobile phase followed a gradient protocol. Water:acetonitrile (0.1% TFA) started at 75:25 (v/v), moved toward 45:55 over 5 min, dropped to 20:80 in 0.1 min, maintained at 20:80 for 2 min, and shifted back to 75:25 in 6 min (13 min run in total). Samples were passed through the Aquasil C18 column (Thermo Scientific 150 mm × 4.6 mm, pore size 5 μm, Waltham, MS) at 1 mL/min and detected at 210 or 256 nm for M2e or cGAMP, respectively.

2.6. Release profiles of cGAMP-loaded MPs of varying CACs

cGAMP-loaded MPs of varying CACs were resuspended in triplicate in either PBS (pH = 7.4) or 0.3 M acetate buffer (pH 5.0) and incubated at 37 °C on a shaker plate (150 rpm). The solution was vortexed to mix at 0.5, 2, 4, 7, 24, 48, 72, and 168 hours before an aliquot was collected. The aliquots were centrifuged at 24,000 × g for 15 min. At hour 168, an aliquot was removed from the vortexed solution and any remaining MPs were dissolved with ethanol. This sample represented the total amount of cGAMP (100% release). Samples were lyophilized and then dissolved in the initial HPLC mobile phase (water:acetonitrile (75:25, v/v) with 0.1% TFA) for cGAMP quantification. The percentage of cGAMP release was calculated based on the absorbance signal for complete degradation of the respective MP set at the last time point.

2.7. In vivo vaccination

Female, BALB/c mice (6–8 weeks old) were obtained from Charles River Laboratories (Wilmington, MA) and kept at a University of North Carolina-Chapel Hill (UNC) facility accredited by the Association for Assessment and Accreditation of Laboratory Animal Care

International. Mice were immunized on Day 0 and 21 with different treatments under a protocol approved by the UNC Institutional Animal Care and Use Committee. To test humoral responses post vaccination, immunization groups included PBS, soluble M2e (solM2e, the consensus peptide SLLTEVETPIRNEWGCRCNDSSD), solM2e with blank MPs, solM2e with MF59-like AddaVax squalene emulsion, solM2e with cGAMP MPs of various CACs (20%, 40%, or 60%), and a combination of M2e MPs of various CACs (20%, 40%, or 60%) with cGAMP MPs of various CACs (20%, 40%, or 60%) (Table S1). To test humoral and cellular responses as well as animal survival upon viral challenge, different immunizations were administered, including PBS, solM2e, solM2e with squalene emulsion, solM2e with cGAMP MPs (60%), M2e MPs of various CACs (20%, 40%, or 60%) with cGAMP MPs (60%), and MPs containing both M2e and cGAMP (M2e/cGAMP MPs (60%)) (Table S2). The same amount of M2e (10 μg) or cGAMP (1 μg) was administered by adjusting the particle dose. Blank MPs were delivered at the same dose as the highest amount of particles needed to deliver the M2e and cGAMP doses. The AddaVax squalene emulsion was mixed 1:1 with solM2e in sterile PBS per the manufacturer's protocol, and all MP groups were resuspended in sterile PBS immediately prior to intramuscular injection (50 μL) into the caudal thigh muscle. Previously we have shown that encapsulated cGAMP is significantly more effective than soluble cGAMP, so in this study it was not used as a control [11].

2.8. Antibody titer analysis

Sera were collected via submandibular bleeding on Day −7, 14, 28, 42, and 70 (time relative to prime injection). The samples were processed by centrifugation at 1,500 × g for 10 min at 4 °C and analyzed for anti-M2e IgG, IgG1, and IgG2a antibody titer. High-affinity 96-well plates were coated with 5 μg/mL M2e overnight. After being washed three times with 0.05% Tween 20 in PBS, plates were blocked with 3% w/v bovine serum albumin (BSA) for 1 hour at room temperature, followed by three more washes. Dilutions of serum samples were added and incubated for 2 hr at room temperature. After three washes, HRP-conjugated anti-IgG, anti-IgG1, or anti-IgG2a secondary antibody (Southern Biotech, Birmingham, AL) was applied for a 1 hr incubation. 3,3′,5,5′-tetramethylbenzidine (TMB) solution was added to each well after three washes, and the plates were developed for 6 min before 1 M sulfuric acid was added. Absorbance at 450 nm was measured with a 630 nm background correction. Antibody titers were determined to be the highest dilution factor that generated signals greater than three times the value of the buffer-alone control.

2.9. Ex vivo antigen recall analysis

Mice were euthanized on Day 28 post prime vaccination, spleens were harvested, and single cell suspension splenocytes were cultured in a 96-well plate (1×106 cells per well) at 37 °C with 5% CO_2 and 100% relative humidity. Splenocytes were stimulated with 10 μg/mL M2e for 24 hours, before supernatants were analyzed for interferon (IFN)-γ, interleukin (IL)2, and IL-6 production via ELISA following the manufacturer's protocol (eBioscience, San Diego, CA). The background signal for media-treated cells were subtracted from all groups when calculating cytokine concentration.

An enzyme-linked immunosorbent spot (ELISpot) assay was conducted using a separate population of harvested splenocytes. Cells were cultured in pre-coated 96-well plates and stimulated with 10 μg/mL M2e for 24 hours, before the number of IFN-γ and IL-2 producing cells were determined per the manufacturer's protocol (eBioscience, San Diego, CA). Background levels for un-stimulated cells were subtracted from all groups.

2.10. Virus titration, influenza viral challenge, and mouse survival analysis

PR8 stock titers were determined by standard focus forming assay. Briefly, serial dilutions of stock were inoculated onto Mandin-Darby Canine Kidney (MDCK; ATCC® CCL-34™) cells and incubated in the presence of an Avicel (FMC BioPolymer) based overlay. Plates were then fixed, and viral foci were detected immunocytochemically via sequential incubation with anti-influenza A nucleoprotein clones A1 and A3, a HPR conjugated goat anti-mouse IgG (KPL) and TrueBlue™ peroxidase substrate (KPL). Viral stock titers were expressed as focus forming units per mL (FFU/mL).

Mice were immunized as stated above and challenged on Day 56 after the prime vaccination. Animals were anesthetized with intraperitoneally injected Avertin (0.15–0.2 mL), which was sterile filtered (0.2 μm) and contained 2–2-2 tribromoethanol (40 mg/mL) and 2-methyl-2-butanol (4% v/v) in PBS. PR8 virus (10,000 ffu) was administered via intranasal infection (20 μL) followed by a secondary PBS instillation (10 μL) to assist in complete delivery to the lungs. Animal weight and monitoring of body condition (e.g., animal activity) was assessed daily for 14 days. A 20% loss of body weight or a moribund body condition were used as survival endpoints.

2.11. Evaluation for cross reactivity against different peptide sequences

Sera were collected on Day −7, 14, 28, 42, and 70 relative to the prime vaccination. Samples were processed as stated earlier and analyzed for IgG, IgG1, and IgG2a antibody titers against the three additional M2e sequences corresponding to A/Puerto Rico/8/34 (H1N1), A/Victoria/3/75 (H3N2), A/Hebei/19/95 (H3N2), A/Thailand/SP-83/04 (H5N1), and A/Vietnam/1203/2004 (H5N1).

2.12. Statistical analysis

Statistical analyses were performed using GraphPad Prism software (La Jolla, CA) with groups indicated in figures. All data points were included in calculations of means or statistical significance, which was defined with a p-value of less than 0.05. Representative results from statistical tests can be found in Supporting Information.

3. Results and Discussion

3.1. Ace-DEX MPs enables tunable release of encapsulated cargos

Encapsulation efficiency and final weight loading of M2e- and/or cGAMP-loaded Ace-DEX MPs are listed in Figure 1A. M2e encapsulation efficiencies were comparable to previously reported studies formulating M2e-expressing vesicular structures, such as viruslike particles (50–54%) [51] or bacterial outer membrane vesicles (38%) [52], within poly (lactic-co-glycolic acid) (PLGA) particles made by similar double emulsion methods. The cGAMP

EEs were also similar to other cGAMP-loaded polymeric particles [11, 19, 21] and substantially higher than liposomal formulations encapsulating CDNs [22–24, 53]. Blank, M2e-, and cGAMP-loaded MPs of various CACs shared similar size, zeta potential, and morphology (Figures 1A, 1B, and S1). Average diameters of all MP sets fell within the range appropriate for phagocytosis by antigen presenting cells (0.2–3 μm) [54–56], and were not statistically different from each other.

Because cGAMP is highly hydrophilic, likely forcing rapid diffusion from drug delivery vehicles, we wanted to investigate the ability to tune its release kinetics from Ace-DEX MPs of various CACs. Faster cGAMP release was observed from MPs of lower CAC under both neutral and acidic pH conditions (Figure 2 and Table S3). At pH 7.4, 20% CAC MPs exhibited a 77.3% burst cGAMP release, compared to a 60.4 or 39.4% burst for the 40 or 60% CAC MPs. The 20% CAC MPs reached 100% release by 24 hours, while 69 or 46% drug was released from the other MPs by the same timepoint. The inverse relationship between adjuvant burst release and MP CAC is likely attributed to the lower CAC MPs' faster greater degradation rate. Ace-DEX of lower CAC contains a higher relative ratio of the kinetic product (acyclic acetal) versus the thermodynamic product (cyclic acetal), thereby degrading more rapidly [33]. This provides the possibility of controlling immune stimulation, which is more advantageous than other cGAMP loaded vehicles that offer little flexibility of release kinetics at neutral pH [19, 21]. The same trend between cGAMP release and MP CAC held true under acidic conditions, where the adjuvant was released much more rapidly than at pH 7.4. This accelerated release was due to acid-sensitive degradability of Ace-DEX MPs, which is advantageous for vaccines as it enables efficient cargo delivery and immune stimulation after lysosomal escape [27]. Similar release profiles of encapsulated cGAMP were previously observed by us when cGAMP was loaded into 40% CAC Ace-DEX MPs formulated via electrohydrodynamic spraying [11]. In that study, approximately 80% or 100% of encapsulated cGAMP was released 4 hours after incubation in neutral or acidic cell media environments, respectively. Similar to the cGAMP Ace-DEX MP release profiles, tunable Ace-DEX MP degradation enables controlled release of various encapsulated cargo [33, 45], suggesting the same holds true for M2e as well.

3.2. Ace-DEX MPs induce controlled humoral responses via tunable antigen and adjuvant delivery

M2e antibody production plays an essential role in generating immunity against influenza [5]. Because Ace-DEX MPs of various CACs enable tunable release of encapsulated cargos, we tested how differential antigen and adjuvant delivery affects the magnitude and kinetics of humoral antibody immune responses. After vaccination with AceDEX MPs of various CACs loaded with M2e and/or cGAMP (Table S1), M2e-specific antibody levels (IgG, IgG1, and IgG2a) were measured. In general, higher antibody titers were observed for mice receiving M2e MPs of higher CACs (Figure 3 and S2, statistics are indicated in Tables S4-6). For instance, IgG, IgG1, and IgG2a levels were all higher for mice vaccinated with M2e MPs (60%) + cGAMP MPs (20%), compared to those receiving M2e MPs (20 or 40%) + cGAMP MPs (20%). The correlative relationship between MP CAC and humoral immunity suggests that M2e MPs of higher CAC, which have longer degradation half-lives [28] and likely more sustained M2e release profiles [45], result in stronger immune

responses compared to the faster degrading MP counterparts. Although the data demonstrates that M2e MP CAC had a fairly pronounced effect on humoral responses, the correlation between antibody titer and cGAMP MP CAC was not as definitive. For example, mice vaccinated with M2e MPs (40%) and cGAMP MPs (40%) had higher mean titers compared to M2e MPs (40%) and cGAMP MPs (60%). Despite this trend, these differences were not statistically significant (Table S4). The data therefore suggests that anti-M2e antibody production was more dependent on antigen release kinetics. The advantage of more sustained antigen delivery is further supported by the observation that all encapsulated M2e groups generated significantly higher antibody titers compared to solM2e administrated either alone, or with blank or cGAMP MPs (Figure 3). This is a similar finding that others have reported when vaccinating with solM2e versus M2e formulated within liposomes [57], onto gold nanoparticles [58], or with M2e-expressing bacterial outer membrane vesicles encapsulated in PLGA MPs [52]. In our study, encapsulated M2e also induced higher Th1-biased IgG2a production compared to solM2e or solM2e administered with MF59-like AddaVax, which may be attributed to enhanced antigen cross-presentation via MP encapsulation [27]. This more balanced Th1/Th2 response is similar to previous findings [59] and particularly beneficial for fighting influenza viral infections [60–63]. Together these findings highlight the Ace-DEX MP delivery platform's strength and corroborate the importance of having more sustained vaccine delivery for inducing strong humoral responses.

It is interesting to note that the relationship between immune activation kinetics and antigen or adjuvant delivery using Ace-DEX MPs with various CACs is different than prior observations. We previously encapsulated the model antigen OVA and adjuvant murabutide within Ace-DEX MPs of varying CACs to examine their effect on humoral response kinetics [45]. When delivering OVA, MPs of lower CAC showed greater antibody production. These discrepancies may be attributed to different kinetics of antigen processing with a protein versus a peptide. Unlike the high CAC cGAMP MPs offering optimal immune activation, the previous Ace-DEX study also demonstrated that murabutide-loaded MPs of lower CAC exhibited higher humoral responses at earlier timepoints, while MPs of higher CAC generated stronger immunity at later timepoints [45]. This could be attributed to activation kinetics of different pathogen recognition receptors (STING versus nucleotide-binding oligomerization domain-containing protein 2) [33, 44]. Furthermore, different mouse strains were also used in these Ace-DEX studies (BALB/c versus C57BL/6), potentially also contributing to the observed variations in immune activation kinetics in relationship to MP CAC. The differences in these comparisons may imply that each antigen and adjuvant have unique rates of processing that would need to be individually optimized for each vaccine, and that a single CAC Ace-DEX MP is not inclusive to all vaccine formulations.

Ace-DEX MP platform continues to exhibit advantages relative to other delivery systems. Similar to previous Ace-DEX studies, co-polymer systems such as PLGA or polyanhydrides have shown diverse results with respect to control over humoral responses. PLGA MPs with slower antigen release rates have outperformed their faster-releasing liposomal counterparts [64], while this trend in antibody responses was not observed between polyanhydride systems [65]. Mixed polymer systems have also been used to achieve tunable immune activation. Feng et al. used a mixture of three MP sets each composed of different PLGA co-

polymers for attempted control of humoral immune responses [66]. Despite increased antibody titers over soluble antigen, there was no clear advantage of the MP mixture over any single MP component alone. Wang et al. showed varied antibody responses of DNA antigen-loaded POE MPs [67]. Although humoral immunity could be adjusted in these studies, this flexibility was based on less straightforward polymer chemistry or blends, or the use of multiple MP sets. Overall, our Ace-DEX MP system continues to act as an exciting platform for achieving tunable humoral activation using a single-polymer formulation.

To further evaluate the importance of distinct kinetics on vaccine antigen and adjuvant delivery, M2e and cGAMP co-encapsulated within the same MPs were compared to the components individually encapsulated within separate vehicles. Because the cohorts vaccinated with M2e MPs (60%) showed the most promising results in the previous experiments, M2e and cGAMP were co-loaded within 60% CAC MPs and mice were vaccinated following the study design found in Table S2. The trend between antibody titer and CAC of M2e MPs was consistent with the previous experiment (Figure 3 and 4), with stronger titers observed for higher CAC. Moreover, Figure 4 suggests a significant advantage of separately encapsulated MPs' (M2e MPs (60%) + cGAMP MPs (60%)) ability to induce potent antibody production (Figures 4 and S3, statistics are indicated in Tables S7-8) in comparison to the co-loaded MPs. This may be due to separately encapsulated MPs reaching a broader cell population, resulting in more robust and broad cellular activation that led to greater downstream antibody production. The advantage of separately encapsulated antigens and adjuvants has also been previously observed by others using non-tunable delivery systems [68–70]. Ilyinskii et al. demonstrated that a model ovalbumin (OVA) antigen delivered in separate particles from the TLR 7/8 agonist R848 demonstrated higher antibody titers. In a similar model system, Kasturi et al. co-encapsulated OVA with both TLR 4 (MPL) and 7 (R837) agonists. They showed inferior antibody responses with the co-encapsulation formulation compared to separately encapsulated OVA and MPL/R837. In another study, separate encapsulation of the HIV antigen gp120 and adjuvants led to greater IgG antibody subtypes than co-encapsulation. In these studies, authors suggested that separate encapsulation also provides a formulation advantage, because it enables modular delivery of two components. Our study would suggest that the tunable Ace-DEX MP platform provides yet another level of modularity.

3.3. Ace-DEX MPs of different CACs promote tailored cellular immunity

Because cellular immune responses are also crucial for establishing immunity against influenza [71], we investigated the ability to maximize these responses using Ace-DEX MPs with various CACs. When re-stimulated with M2e, splenocytes from mice immunized with M2e MPs of higher CACs (40% or 60%) generated significantly higher levels of IFN-γ, IL-2, and IL-6 than mice vaccinated with M2e MPs (20%) (Figure 5A-C). Larger numbers of IFNγ or IL-2 expressing splenocytes were also observed for mice vaccinated with the same M2e MPs (40% or 60%) (Figure 5D and 5E). Furthermore, cellular responses were greatly enhanced for encapsulated compared to soluble M2e and were significantly greater for M2eloaded Ace-DEX MPs versus the benchmark solM2e/MF59-like squalene emulsion formulation. This can be attributed to Ace-DEX MPs' advantageous acid-sensitivity that drives enhanced APC activation [44], antigen cross-presentation [27], and cellular immunity

[67]. This direct correlation between MP CAC and cellular immune responses echoes the trend observed for antibody production. In particular, these results with cellular immunity reflecting the higher IgG2a production observed for slower degrading M2e MPs suggest a more balanced Th1/Th2 response. While others have not investigated how differing M2e release profiles from nano/microcarriers affect cellular responses, vaccines containing M2e particle formulations have similarly demonstrated potent IFN-γ or IL-2 responses [47, 52, 72, 73].

In contrast to the current study, our previous study indicates that lower CAC Ace-DEX MPs encapsulating OVA generated greater cellular immunity [45]. Unlike the high CAC cGAMP MPs offering optimal immune activation, the previous Ace-DEX study also demonstrated that low CAC murabutide-loaded MPs led to higher cellular immunity. Similar to the reasons provided with the humoral immunity discussion, different antigen processing, adjuvant signaling pathways, and mouse strains all could have contributed to the discrepancies. Moreover, this indicates that each antigen and adjuvant require fine-tuning for optimal immune activity.

In addition to showing the strength of M2e formulation for increasing cellular immunity, we also demonstrated that groups immunized with M2e and cGAMP encapsulated within separate MPs generated comparable levels of inflammatory cytokines and numbers of cytokine-expressing cells to the co-loaded MP group (Figure 5). Previous research has suggested that an antigen and adjuvant need to be present in the same endocytic compartment to induce maximal antigen presentation [74]. Other researchers have confirmed this hypothesis by showing more potent T cell responses with co-encapsulation [75]. Our observation agrees with other findings that showed co-encapsulated and separately loaded particles demonstrated similar cellular immunity [41, 68]. Based on these varying results, further studies would be needed to determine whether co-existence of both M2e and cGAMP in the same endocytic compartments are leading to the observed cytokine responses.

3.4. Ace-DEX MPs protect mice against lethal influenza challenge

To evaluate the protective effect of Ace-DEX MP vaccines, mice were challenged with the PR8 influenza virus one month after the boost immunization. The M2e MP + cGAMP MP-vaccinated groups exhibited substantially enhanced survival over the un-immunized PBS control or the benchmark M2e + MF59-like squalene emulsion formulation (Figure 6). Since mice were vaccinated with the M2e consensus peptide, which contains one mismatch to the PR8 sequence, protection against a PR8 challenge suggests some crossreactivity of the M2e and cGAMP MP vaccine. It is also important to note slower-degrading M2e MPs (40% or 60%) exhibited significantly stronger protection compared to the fastdegrading counterpart (M2e MPs (20%)). The more robust protection is likely attributed to the enhanced humoral and cellular immunity observed for M2e MPs (40% or 60%), suggesting the importance of sustained adjuvant and antigen delivery at establishing more protective immunity against influenza infection. Moreover, M2e and cGAMP encapsulated within separate MP vehicles (M2e MPs (40% or 60%) + cGAMP MPs (60%)) showed substantially higher protective efficacy than the co-loaded group, which was in accordance with the enhanced antibody and

cytokine production observed (Figure 4 and 5). This is because a combination of strong humoral and cellular responses is likely required for successful protection against the flu [4]. Superior protection with separately encapsulated antigen and adjuvant was also previously observed by us in a preclinical Anthrax model [59].

The observed protection against PR8 is comparable to other published studies using M2e delivery vehicles. In one of these studies, a hydrophobic moiety-modified consensus M2e was co-encapsulated with MPL in liposomes [72]. In two other studies, Tao et al. used a chemically-modified M2e conjugated to gold nanoparticles and adjuvanted them with soluble CpG [58, 76]. Other M2e delivery systems [52, 73, 77] also demonstrated similar protection, but like the other studies did not offer modulation of immune response kinetics. Furthermore, they had significantly different experimental designs than our study, emphasizing the robustness of the current challenge model. The studies required either two booster injections, went by less stringent survival criteria (25% vs. 20% weight loss), included multiple conserved antigens, and/or had less robust challenge models (PBS-immunized controls with much longer median survival times). Some of their challenge experiments were also performed sooner (7, 14, or 21 days after the boost) compared to our study (28 days following the boost), which indicates potentially more prolonged protective ability of the Ace-DEX MP vaccines.

3.5. Sera from vaccinated mice generate cross reactivity against variant M2e sequences

To further examine the potential strength of an Ace-DEX MP vaccine, crossreactivity of antibodies against non-consensus M2e sequences from phylogenetically different flu strains was assessed. When tested against the M2e sequences of A/Puerto Rico/8/34 (H1N1, Group 1) and A/Victoria/3/75 (H3N2, Group 2), which both contain 1 mismatch to the consensus, high antibody titers were observed from sera collected 28 days post prime vaccination (Figure 7). A potent antibody response was also observed when sera were tested against the M2e sequence for A/Hebei/19/95 (H3N2, Group 2), which contains 2 mismatches to the consensus. Finally, when tested against an M2e sequence of 3 mismatches, associated with A/Thailand/SP-83/04 and A/Vietnam/1203/2004 strains (H5N1, Group 1), robust humoral immunity was also demonstrated. Reactivity against sequences from both group 1 and 2 influenza A viruses by Ace-DEX MP vaccines underscores the potency of the formulation, indicating its promising potential as a universal influenza vaccine platform. Besides the substantial cross-reactivity against various M2e sequences, the positive relationship between humoral response and MP CAC was generally true for various M2e antigens tested, further emphasizing the tunable immune activation kinetics for multiple influenza viral strains (Table S9). Co-encapsulated MPs again yielded substantially lower antibody levels, supporting the importance of separate antigen and adjuvant delivery.

Although other researchers have also demonstrated reactivity of immune sera with divergent M2e sequences, our system is advantageous due to more robust responses using just a single M2e sequence for immunization and potentially safer formulations. Fan et al. immunized with multiple M2e sequences associated with several H1N1 or H3N2 strains, and then showed reactivity against sequences containing many mismatches [46]. Although Tompkins et al. vaccinated with the consensus M2e and showed some cross-reactivity against M2e

sequences with either 1 or 3 mismatches, the reactivity against the 3-mismatch H5N1 strain M2e sequences was much less robust than the H1N1 PR8 M2e sequence [48]. Mice in both of these studies were also vaccinated with reactogenic Complete Freund's adjuvant and Incomplete Freund's adjuvant [78], which cannot be applied in humans due to their toxicity. While others have demonstrated vaccine robustness by showing antibody reactivity against various whole flu viruses, multiple M2e sequences were used for immunization [73, 79].

4. Conclusions

We demonstrate M2e- and cGAMP-encapsulated Ace-DEX MPs induce robust humoral and cellular immune responses and provide effective protection against a lethal influenza infection in a mouse model. The Ace-DEX MP delivery platform enables controlled activation of both humoral and cellular responses. MPs offering more sustained release profiles (60% CAC) trended towards higher antibody titers, cytokine production, a greater number of inflammatory-cytokine producing cells, and the most protection against a viral challenge. Considering the significant effect of flexible, distinct control over immune activation, the Ace-DEX platform allows for optimization of the kinetics and magnitude of protective immunity for the disease of interest. This enables the potential for improved safety and efficacy of subunit vaccines. To the best of our knowledge, we are the first group to show the impact of tunable immune activation via a biomaterial-based delivery platform on animal survival following a lethal pathogen challenge. Moreover, antibodies generated because of vaccination are cross-reactive against variant antigens from different virus origins, suggesting these vaccines could provide universal protection. Kinetics of immune activation and its role in different disease models will be explored in the future to facilitate our understanding of controlled vaccine delivery. Different challenge models will also be explored to further support the potential universal protective efficacy of the Ace-DEX MP vaccine.

Supplementary Material

Refer to Web version on PubMed Central for supplementary material.

Acknowledgements

This work was supported by Internal Funds of the University of North Carolina at Chapel Hill and the National Institutes of Health 5U19AI109784-03. We thank Drs. Sai Archana Krovi and Robert D. Junkins for their help with *in vivo* experiments. Influenza virus and stock titer quantification were provided by the Virology Unit of the Duke Regional Biocontainment Laboratory (RBL) under the management of Dr. Charles E. McGee and directorship of Dr. Gregory D. Sempowski, which received partial support for construction from the National Institutes of Health, National Institute of Allergy and Infectious Diseases (UC6-AI058607). We gratefully acknowledge the technical support of Christopher Sample and Kimberly Parks. The following reagent was obtained through BEI Resources, NIAID, NIH: Monoclonal Anti-Influenza A Virus Nucleoprotein (NP), Clones A1 and A3 (ascites blend, Mouse), NR-4282. The authors would also like to thank the UNC CFAR Virology, Immunology, and Microbiology Core for the use of their ELISpot reader. This work was performed in part at the Chapel Hill Analytical and Nanofabrication Laboratory, CHANL, a member of the North Carolina Research Triangle Nanotechnology Network, RTNN, which is supported by the National Science Foundation, Grant ECCS-1542015, as part of the National Nanotechnology Coordinated Infrastructure, NNCI.

References

1. Disease Burden of Influenza. 2017 [cited 2018 Feb 20]; Available from: https://www.cdc.gov/flu/about/disease/burden.htm.
2. Molinari NA, et al., The annual impact of seasonal influenza in the US: measuring disease burden and costs. Vaccine, 2007 25(27): p. 5086–96. [PubMed: 17544181]
3. Belongia EA, et al., Effectiveness of inactivated influenza vaccines varied substantially with antigenic match from the 2004–2005 season to the 2006–2007 season. J Infect Dis, 2009 199(2): p. 159–67. [PubMed: 19086915]
4. Deng L, et al., M2e-Based Universal Influenza A Vaccines. Vaccines (Basel), 2015 3(1): p. 105–36. [PubMed: 26344949]
5. Neirynck S, et al., A universal influenza A vaccine based on the extracellular domain of the M2 protein. Nat Med, 1999 5(10): p. 1157–63. [PubMed: 10502819]
6. Pashine A, Valiante NM, and Ulmer JB, Targeting the innate immune response with improved vaccine adjuvants. Nat Med, 2005 11(4 Suppl): p. S63–8. [PubMed: 15812492]
7. Tagliabue A and Rappuoli R, Vaccine adjuvants: the dream becomes real. Hum Vaccin, 2008 4(5): p. 347–9. [PubMed: 18682690]
8. Campbell JD, Development of the CpG Adjuvant 1018: A Case Study. Methods Mol Biol, 2017 1494: p. 15–27. [PubMed: 27718183]
9. Bungener L, et al., Alum boosts TH2-type antibody responses to whole-inactivated virus influenza vaccine in mice but does not confer superior protection. Vaccine, 2008 26(19): p. 2350–9. [PubMed: 18400340]
10. Dubensky TW, Jr., Kanne DB, and Leong ML, Rationale, progress and development of vaccines utilizing STING-activating cyclic dinucleotide adjuvants. Ther Adv Vaccines, 2013 1(4): p. 131–43. [PubMed: 24757520]
11. Junkins RD, et al., A robust microparticle platform for a STING-targeted adjuvant that enhances both humoral and cellular immunity during vaccination. J Control Release, 2018 270: p. 1–13. [PubMed: 29170142]
12. Wang J, Li P, and Wu MX, Natural STING Agonist as an “Ideal” Adjuvant for Cutaneous Vaccination. J Invest Dermatol, 2016 136(11): p. 2183–2191. [PubMed: 27287182]
13. Sanchez MV, et al., Intranasal delivery of influenza rNP adjuvanted with c-di-AMP induces strong humoral and cellular immune responses and provides protection against virus challenge. PLoS One, 2014 9(8): p. e104824. [PubMed: 25140692]
14. Major D, et al., Intranasal vaccination with a plant-derived H5 HA vaccine protects mice and ferrets against highly pathogenic avian influenza virus challenge. Hum Vaccin Immunother, 2015 11(5): p. 1235–43. [PubMed: 25714901]
15. Madhun AS, et al., Intranasal c-di-GMP-adjuvanted plant-derived H5 influenza vaccine induces multifunctional Th1 CD4+ cells and strong mucosal and systemic antibody responses in mice. Vaccine, 2011 29(31): p. 4973–82. [PubMed: 21600260]
16. Pedersen GK, et al., Evaluation of the sublingual route for administration of influenza H5N1 virosomes in combination with the bacterial second messenger cdi-GMP. PLoS One, 2011 6(11): p. e26973. [PubMed: 22069479]
17. Svindland SC, et al., A study of Chitosan and c-di-GMP as mucosal adjuvants for intranasal influenza H5N1 vaccine. Influenza Other Respir Viruses, 2013 7(6): p. 1181–93. [PubMed: 23170900]
18. Neuhaus V, et al., A new adjuvanted nanoparticle-based H1N1 influenza vaccine induced antigen-specific local mucosal and systemic immune responses after administration into the lung. Vaccine, 2014 32(26): p. 3216–22. [PubMed: 24731807]
19. Aroh C, et al., Innate Immune Activation by cGMP-AMP Nanoparticles Leads to Potent and Long-Acting Antiretroviral Response against HIV-1. J Immunol, 2017 199(11): p. 3840–3848. [PubMed: 29084836]
20. Wilson DR, et al., Biodegradable STING agonist nanoparticles for enhanced cancer immunotherapy. Nanomedicine, 2017 14(2): p. 237–246. [PubMed: 29127039]

21. Lee E, et al., Submicron-sized hydrogels incorporating cyclic dinucleotides for selective delivery and elevated cytokine release in macrophages. Acta Biomater, 2016 29: p. 271–281. [PubMed: 26485167]
22. Miyabe H, et al., A new adjuvant delivery system 'cyclic di-GMP/YSK05 liposome' for cancer immunotherapy. J Control Release, 2014 184: p. 20–7. [PubMed: 24727060]
23. Hanson MC, et al., Nanoparticulate STING agonists are potent lymph nodetargeted vaccine adjuvants. J Clin Invest, 2015 125(6): p. 2532–46. [PubMed: 25938786]
24. Goodwin TJ and Huang L, Investigation of phosphorylated adjuvants coencapsulated with a model cancer peptide antigen for the treatment of colorectal cancer and liver metastasis. Vaccine, 2017 35(19): p. 2550–2557. [PubMed: 28385609]
25. Koshy ST, et al., Liposomal Delivery Enhances Immune Activation by STING Agonists for Cancer Immunotherapy. Advanced Biosystems, 2017 1(1–2).
26. Bachelder EM, et al., Acetal-derivatized dextran: an acid-responsive biodegradable material for therapeutic applications. J Am Chem Soc, 2008 130(32): p. 10494–5. [PubMed: 18630909]
27. Broaders KE, et al., Acetalated dextran is a chemically and biologically tunable material for particulate immunotherapy. Proc Natl Acad Sci U S A, 2009 106(14): p. 5497–502. [PubMed: 19321415]
28. Kauffman KJ, et al., Synthesis and characterization of acetalated dextran polymer and microparticles with ethanol as a degradation product. ACS Appl Mater Interfaces, 2012 4(8): p. 4149–55. [PubMed: 22833690]
29. Kanthamneni N, et al., Enhanced stability of horseradish peroxidase encapsulated in acetalated dextran microparticles stored outside cold chain conditions. Int J Pharm, 2012 431(1–2): p. 101–10. [PubMed: 22548844]
30. Kohane DS, Microparticles and nanoparticles for drug delivery. Biotechnol Bioeng, 2007 96(2): p. 203–9. [PubMed: 17191251]
31. Duong AD, et al., Electrospray encapsulation of toll-like receptor agonist resiquimod in polymer microparticles for the treatment of visceral leishmaniasis. Mol Pharm, 2013 10(3): p. 1045–55. [PubMed: 23320733]
32. Chen N, et al., Co-Delivery of Disease Associated Peptide and Rapamycin via Acetalated Dextran Microparticles for Treatment of Multiple Sclerosis. Advanced Biosystems, 2017 1(3): p. 12.
33. Chen N, et al., Degradation of acetalated dextran can be broadly tuned based on cyclic acetal coverage and molecular weight. Int J Pharm, 2016 512(1): p. 147–157. [PubMed: 27543351]
34. Gupta P, et al., Degradation of poly(beta-amino ester) gels in alcohols through transesterification: A method to conjugate drugs to polymer matrices. J Polym Sci A Polym Chem, 2017 55(12): p. 2019–2026. [PubMed: 29398778]
35. Qiao ZY, et al., Multi-responsive nanogels containing motifs of ortho ester, oligo(ethylene glycol) and disulfide linkage as carriers of hydrophobic anti-cancer drugs. J Control Release, 2011 152(1): p. 57–66. [PubMed: 21392550]
36. Yang SC, et al., Polyketal copolymers: a new acid-sensitive delivery vehicle for treating acute inflammatory diseases. Bioconjug Chem, 2008 19(6): p. 1164–9. [PubMed: 18500834]
37. Brice GT, et al., Extended immunization intervals enhance the immunogenicity and protective efficacy of plasmid DNA vaccines. Microbes Infect, 2007 9(12–13): p. 1439–46. [PubMed: 17913540]
38. Ledgerwood JE, et al., Prime-boost interval matters: a randomized phase 1 study to identify the minimum interval necessary to observe the H5 DNA influenza vaccine priming effect. J Infect Dis, 2013 208(3): p. 418–22. [PubMed: 23633407]
39. Iezzi G, Karjalainen K, and Lanzavecchia A, The duration of antigenic stimulation determines the fate of naive and effector T cells. Immunity, 1998 8(1): p. 89–95. [PubMed: 9462514]
40. Obst R, The Timing of T Cell Priming and Cycling. Front Immunol, 2015 6: p. 563. [PubMed: 26594213]
41. Wang Q, et al., Time course study of the antigen-specific immune response to a PLGA microparticle vaccine formulation. Biomaterials, 2014 35(29): p. 8385–93. [PubMed: 24986256]

42. Zinkernagel RM, et al., Antigen localisation regulates immune responses in a dose- and time-dependent fashion: a geographical view of immune reactivity. Immunol Rev, 1997 156: p. 199–209. [PubMed: 9176709]
43. Zinkernagel RM, Localization dose and time of antigens determine immune reactivity. Semin Immunol, 2000 12(3): p. 163–71; discussion 257–344. [PubMed: 10910735]
44. Peine KJ, et al., Efficient delivery of the toll-like receptor agonists polyinosinic:polycytidylic acid and CpG to macrophages by acetalated dextran microparticles. Mol Pharm, 2013 10(8): p. 2849–57. [PubMed: 23768126]
45. Chen N, et al., Tunable degradation of acetalated dextran microparticles enables controlled vaccine adjuvant and antigen delivery to modulate adaptive immune responses. J Control Release, 2018 273: p. 147–159. [PubMed: 29407676]
46. Fan J, et al., Preclinical study of influenza virus A M2 peptide conjugate vaccines in mice, ferrets, and rhesus monkeys. Vaccine, 2004 22(23–24): p. 2993–3003. [PubMed: 15297047]
47. Tao W, et al., Consensus M2e peptide conjugated to gold nanoparticles confers protection against H1N1, H3N2 and H5N1 influenza A viruses. Antiviral Res, 2017 141: p. 62–72. [PubMed: 28161578]
48. Tompkins SM, et al., Matrix protein 2 vaccination and protection against influenza viruses, including subtype H5N1. Emerg Infect Dis, 2007 13(3): p. 426–35. [PubMed: 17552096]
49. GenScript Peptide Property Calculator. [cited 2018 September]; Available from: https://www.genscript.com/tools/peptide-property-calculator.
50. Brito LA and Singh M, Acceptable levels of endotoxin in vaccine formulations during preclinical research. J Pharm Sci, 2011 100(1): p. 34–7. [PubMed: 20575063]
51. Hiremath J, et al., Entrapment of H1N1 Influenza Virus Derived Conserved Peptides in PLGA Nanoparticles Enhances T Cell Response and Vaccine Efficacy in Pigs. PLoS One, 2016 11(4): p. e0151922. [PubMed: 27093541]
52. Watkins HC, et al., A single dose and long lasting vaccine against pandemic influenza through the controlled release of a heterospecies tandem M2 sequence embedded within detoxified bacterial outer membrane vesicles. Vaccine, 2017 35(40): p. 5373–5380. [PubMed: 28866291]
53. Nakamura T, et al., Liposomes loaded with a STING pathway ligand, cyclic di-GMP, enhance cancer immunotherapy against metastatic melanoma. J Control Release, 2015 216: p. 149–57. [PubMed: 26282097]
54. Manolova V, et al., Nanoparticles target distinct dendritic cell populations according to their size. Eur J Immunol, 2008 38(5): p. 1404–13. [PubMed: 18389478]
55. Champion JA, Walker A, and Mitragotri S, Role of particle size in phagocytosis of polymeric microspheres. Pharm Res, 2008 25(8): p. 1815–21. [PubMed: 18373181]
56. Gamvrellis A, et al., Vaccines that facilitate antigen entry into dendritic cells. Immunol Cell Biol, 2004 82(5): p. 506–16. [PubMed: 15479436]
57. Ernst WA, et al., Protection against H1, H5, H6 and H9 influenza A infection with liposomal matrix 2 epitope vaccines. Vaccine, 2006 24(24): p. 5158–68. [PubMed: 16713037]
58. Tao W, Ziemer KS, and Gill HS, Gold nanoparticle-M2e conjugate coformulated with CpG induces protective immunity against influenza A virus. Nanomedicine (Lond), 2014 9(2): p. 237–51. [PubMed: 23829488]
59. Gallovic MD, et al., Acetalated Dextran Microparticulate Vaccine Formulated via Coaxial Electrospray Preserves Toxin Neutralization and Enhances Murine Survival Following Inhalational Bacillus Anthracis Exposure. Adv Healthc Mater, 2016 5(20): p. 2617–2627. [PubMed: 27594343]
60. Mantile F, et al., Alum and squalene-oil-in-water emulsion enhance the titer and avidity of anti-Abeta antibodies induced by multimeric protein antigen (1–11)E2, preserving the Igg1-skewed isotype distribution. PLoS One, 2014 9(7): p. e101474. [PubMed: 24983378]
61. Magor KE, et al., One gene encodes the heavy chains for three different forms of IgY in the duck. J Immunol, 1994 153(12): p. 5549–55. [PubMed: 7989756]
62. Song A, et al., Evaluation of a fully human monoclonal antibody against multiple influenza A viral strains in mice and a pandemic H1N1 strain in nonhuman primates. Antiviral Res, 2014 111: p. 60–8. [PubMed: 25218949]

63. Guilliams M, et al., The function of Fcgamma receptors in dendritic cells and macrophages. Nat Rev Immunol, 2014 14(2): p. 94–108. [PubMed: 24445665]
64. Demento SL, et al., Role of sustained antigen release from nanoparticle vaccines in shaping the T cell memory phenotype. Biomaterials, 2012 33(19): p. 4957–64. [PubMed: 22484047]
65. Petersen LK, et al., Amphiphilic polyanhydride nanoparticles stabilize Bacillus anthracis protective antigen. Mol Pharm, 2012 9(4): p. 874–82. [PubMed: 22380593]
66. Feng L, et al., Pharmaceutical and immunological evaluation of a single-dose hepatitis B vaccine using PLGA microspheres. J Control Release, 2006 112(1): p. 35–42. [PubMed: 16516999]
67. Wang C, et al., Molecularly engineered poly(ortho ester) microspheres for enhanced delivery of DNA vaccines. Nat Mater, 2004 3(3): p. 190–6. [PubMed: 14991022]
68. Ilyinskii PO, et al., Adjuvant-carrying synthetic vaccine particles augment the immune response to encapsulated antigen and exhibit strong local immune activation without inducing systemic cytokine release. Vaccine, 2014 32(24): p. 2882–95. [PubMed: 24593999]
69. Kasturi SP, et al., Programming the magnitude and persistence of antibody responses with innate immunity. Nature, 2011 470(7335): p. 543–7. [PubMed: 21350488]
70. Kazzaz J, et al., Encapsulation of the immune potentiators MPL and RC529 in PLG microparticles enhances their potency. J Control Release, 2006 110(3): p. 566–73. [PubMed: 16360956]
71. Thomas PG, et al., Cell-mediated protection in influenza infection. Emerg Infect Dis, 2006 12(1): p. 48–54. [PubMed: 16494717]
72. Adler-Moore J, et al., Characterization of the murine Th2 response to immunization with liposomal M2e influenza vaccine. Vaccine, 2011 29(27): p. 4460–8. [PubMed: 21545821]
73. Deng L, et al., Double-layered protein nanoparticles induce broad protection against divergent influenza A viruses. Nat Commun, 2018 9(1): p. 359. [PubMed: 29367723]
74. Schlosser E, et al., TLR ligands and antigen need to be coencapsulated into the same biodegradable microsphere for the generation of potent cytotoxic T lymphocyte responses. Vaccine, 2008 26(13): p. 1626–37. [PubMed: 18295941]
75. Blander JM and Medzhitov R, Toll-dependent selection of microbial antigens for presentation by dendritic cells. Nature, 2006 440(7085): p. 808–12. [PubMed: 16489357]
76. Tao W and Gill HS, M2e-immobilized gold nanoparticles as influenza A vaccine: Role of soluble M2e and longevity of protection. Vaccine, 2015 33(20): p. 2307–15. [PubMed: 25842219]
77. Deng L, et al., Protection against Influenza A Virus Challenge with M2e-Displaying Filamentous Escherichia coli Phages. PLoS One, 2015 10(5): p. e0126650. [PubMed: 25973787]
78. Jackson LR and Fox JG, Institutional Policies and Guidelines on Adjuvants and Antibody Production. ILAR J, 1995 37(3): p. 141–152. [PubMed: 11528034]
79. Kim MC, et al., Virus-like particles containing multiple M2 extracellular domains confer improved cross-protection against various subtypes of influenza virus. Mol Ther, 2013 21(2): p. 485–92. [PubMed: 23247101]

A

Vaccine Formulation	Mean Diameter (nm)	Polydispersity Index	Zeta Potential (mV)	Encapsulation Efficiency (%)		Final Weight Loading (μg Cargo / mg MPs)	
				M2e	cGAMP	M2e	cGAMP
Blank MPs	747 ± 72.5	0.405	-10.4	-	-	-	-
M2e MPs (20%)	727 ± 228	0.486	-11.1	53.8 ± 8.0	-	2.7 ± 0.4	-
M2e MPs (40%)	706 ± 145	0.415	-12.1	42.6 ± 3.6	-	2.1 ± 0.2	-
M2e MPs (60%)	622 ± 94.5	0.326	-8.3	67.6 ± 1.6	-	3.4 ± 0.1	-
cGAMP MPs (20%)	1003 ± 298	0.400	-14.3	-	77.8 ± 8.7	-	3.9 ± 0.4
cGAMP MPs (40%)	652 ± 260	0.366	-8.4	-	40.8 ± 8.0	-	2.0 ± 0.4
cGAMP MPs (60%)	678 ± 217	0.415	-12.1	-	42.8 ± 7.7	-	2.1 ± 0.4
M2e/cGAMP MPs (60%)	650 ± 81.2	0.407	-12.6	58.6 ± 1.5	58.8 ± 4.7	2.9 ± 0.1	0.3 ± 0.2

B

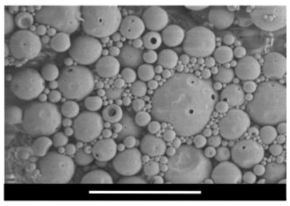

Figure 1.

(A) Mean diameter, polydispersity index, zeta potential, encapsulation efficiencies, and final weight loading for M2e or cGAMP-loaded acetalated dextran (Ace-DEX) microparticles (MPs) and (B) a representative scanning electron micrograph of the MPs. Percentages indicate the MPs' relative cyclic acetal coverage. The last row in the table indicates co-encapsulated MPs. Number-weighted mean hydrodynamic diameters are presented as average ± standard deviation of five technical replicates (n = 5). Scale bar is 5 μm.

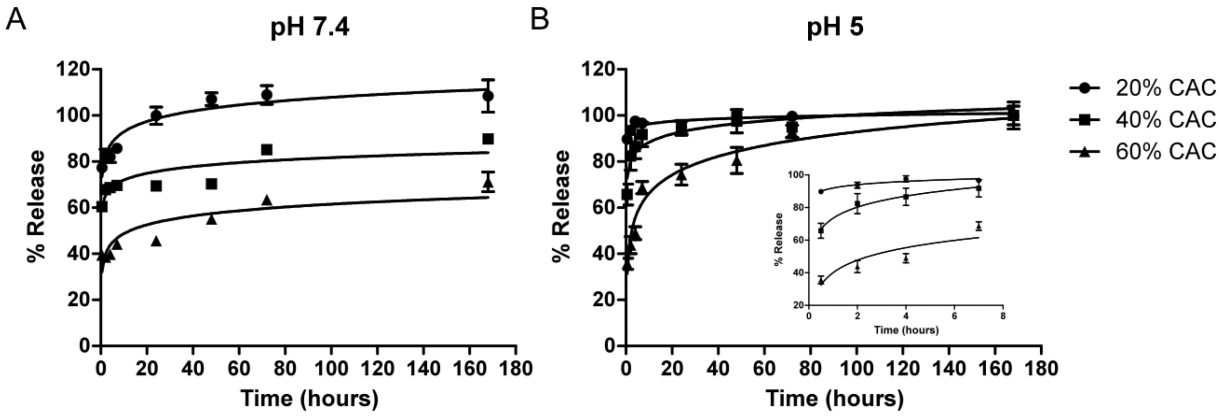

Figure 2.

cGAMP release profiles at (A) pH 7.4 and (B) pH 5.0 of microparticles formulated from acetalated dextran of different relative cyclic acetal coverages (CACs, presented as percentages in figure legend). The inset in panel (B) displays the first 8 hours of release. Data are presented as mean ± standard error of the mean (n = 3). The solid lines are logarithmic fits added as a visual guide.

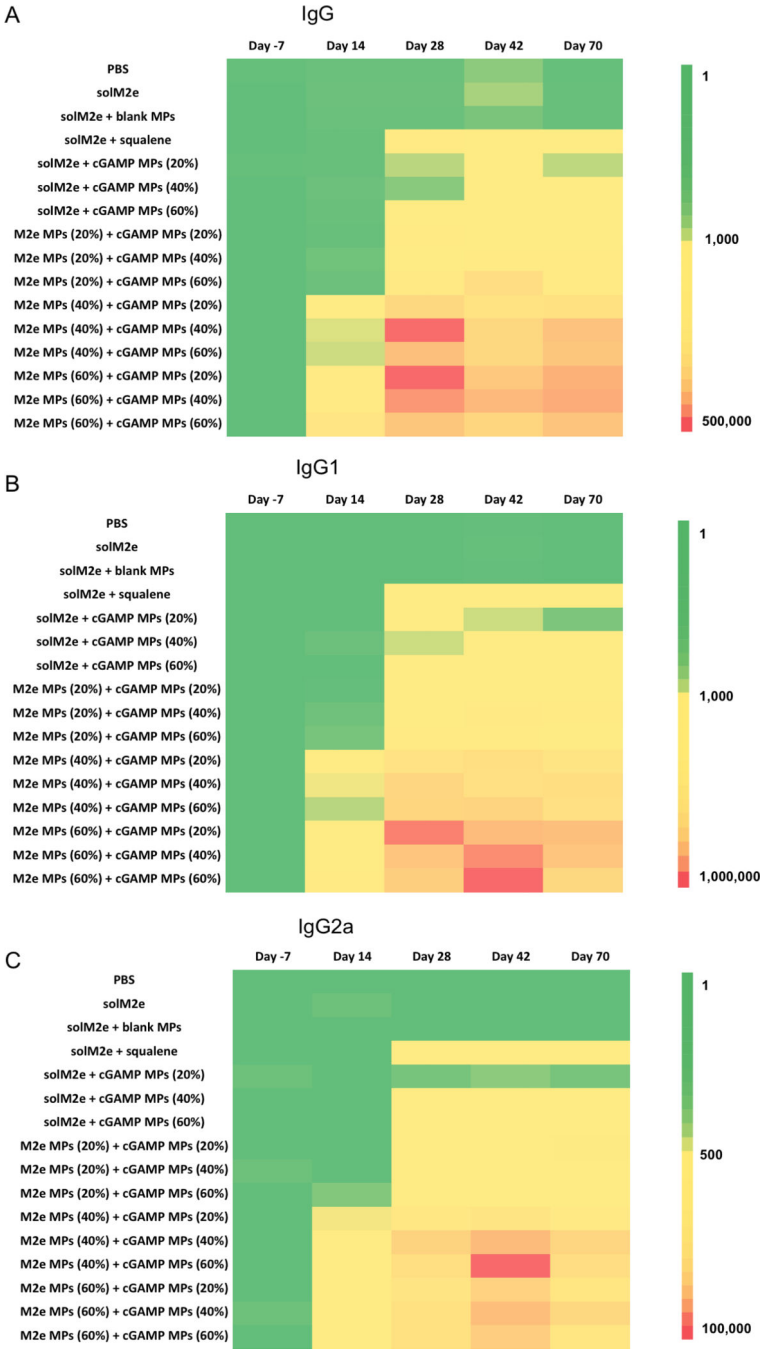

Figure 3.

Heat maps of anti-M2e (A) total IgG, (B) IgG1, and (C) IgG2a antibody titers of mice vaccinated on Day 0 and 21 with phosphate-buffered saline (PBS), soluble M2e (solM2e), solM2e + MF59-like AddaVax (solM2e + squalene), solM2e + blank microparticles (MPs), solM2e + cGAMP-loaded MPs (cGAMP MPs (20, 40, or 60%)), or M2e-loaded MPs (M2e MPs (20, 40, or 60%)) + cGAMP-loaded MPs (cGAMP MPs (20, 40, or 60%)) (n = 5). All MPs were composed of acetalated dextran (Ace-DEX), and percentages indicate Ace-DEX MP relative cyclic acetal coverages. Particle amount was adjusted to administer 10 μg M2e

and/or 1 μg cGAMP. Blank MPs (40%) were administered at the same level as the highest amount of MPs needed to deliver the M2e and cGAMP doses.

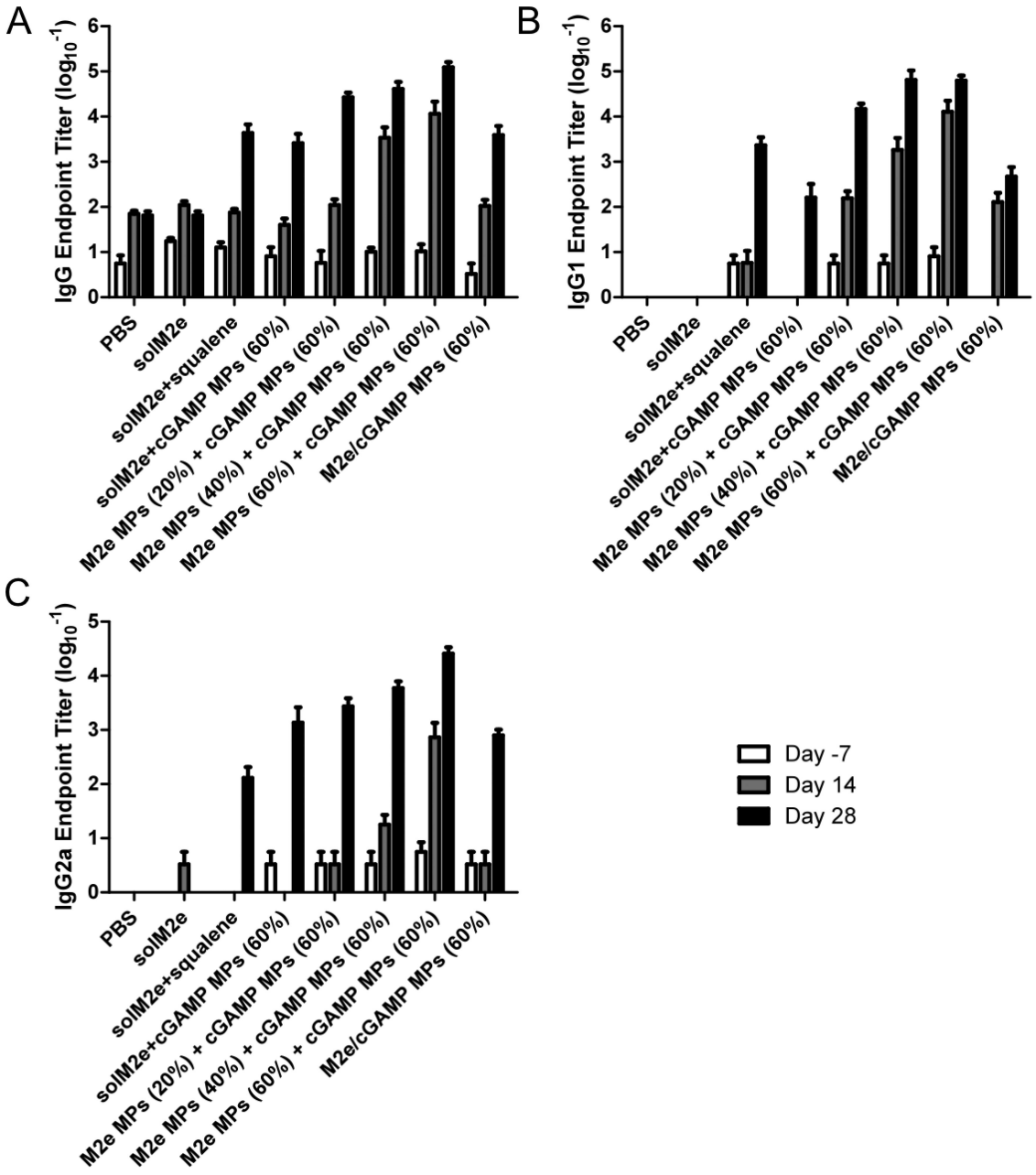

Figure 4.

Anti-M2e (A) total IgG, (B) IgG1, and (C) IgG2a antibody titers of mice vaccinated on Day 0 and 21 with phosphate-buffered saline (PBS), soluble M2e (solM2e), solM2e MF59-like AddaVax (solM2e + squalene), solM2e + cGAMP-loaded microparticles (cGAMP MPs (60%)), M2e-loaded MPs (M2e MPs (20, 40, or 60%)) + cGAMP MPs (60%), or MPs containing both M2e and cGAMP (M2e/cGAMP MPs (60%)) (n = 5). All MPs were composed of acetalated dextran (Ace-DEX), and percentages indicate Ace-DEX MP relative cyclic acetal coverages. MP dose was adjusted to administer 10 μg M2e and/or 1 μg cGAMP.

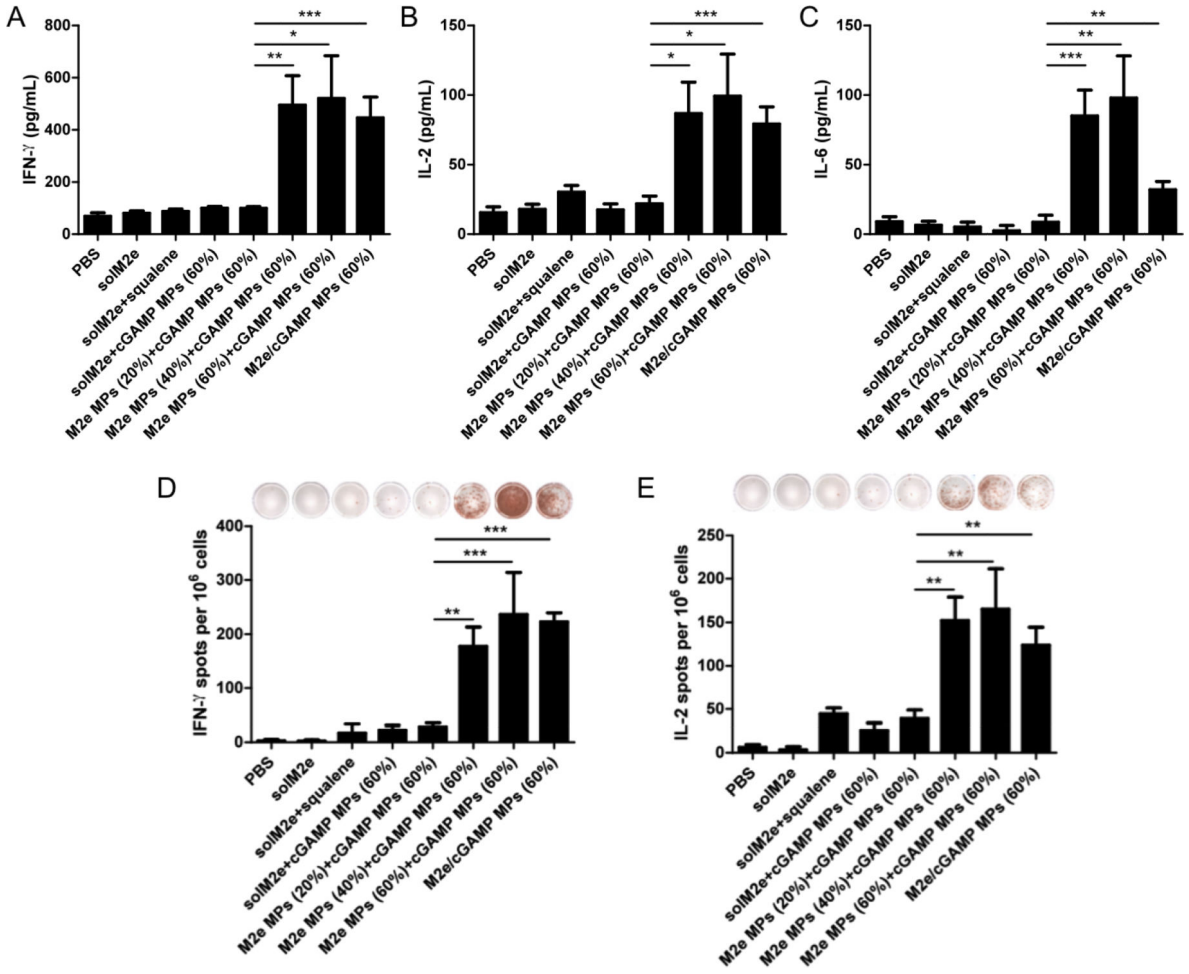

Figure 5.

Mice vaccinated on day 0 and 21 with indicated groups were evaluated for cellular responses. (A-C) Measurements of soluble cytokines after antigen recall: (A) interferon (IFN)-γ, (B) interleukin (IL)-2, and (C) IL-6 production. ELISpots isolated from mice on Day 28 were evaluated for (D) IFN-γ and (E) IL-2 expression. Experimental groups were phosphate-buffered saline (PBS), soluble M2e (solM2e), solM2e + MF59-like AddaVax (solM2e + squalene), M2e-loaded microparticles (M2e MPs (20, 40, or 60%)) + cGAMPloaded MPs (cGAMP MPs (60%)), or MPs containing both M2e and cGAMP (M2e/cGAMP MPs (60%)). All MPs were composed of acetalated dextran (Ace-DEX), and percentages indicate Ace-DEX MP relative cyclic acetal coverages. The M2e and cGAMP doses were 10 μg and 1 μg, respectively. Statistical significance is presented as $*p < 0.05$, $**p < 0.01$, and $***p < 0.001$, performed using a one-way ANOVA. Data are presented as mean ± standard error of the mean (n = 5). Representative images of wells are included in (D, E) for each vaccination group.

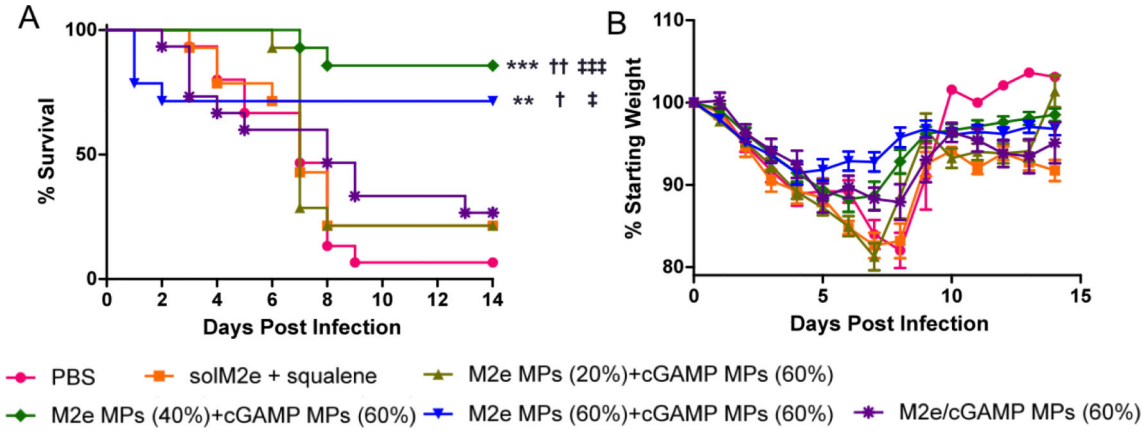

Figure 6.

(A) Survival curve and (B) body weight of mice challenged with 10,000 ffu of A/Puerto Rico/8/1934 H1N1 flu strain. Mice were vaccinated on Day 0 and Day 21 with phosphate-buffered saline (PBS), soluble M2e + MF59-like AddaVax (solM2e + squalene), M2e-loaded microparticles (M2e MPs (20, 40, or 60%)) + cGAMP-loaded microparticles (cGAMP MPs (60%)), or MPs containing both M2e and cGAMP (M2e/cGAMP MPs (60%)). All MPs were composed of acetalated dextran (Ace-DEX), and percentages indicate AceDEX MP relative cyclic acetal coverages. The M2e and cGAMP doses were 10 μg and 1 μg, respectively. Mice were challenged on Day 56, monitored for up to 14 days, and euthanized upon 20% loss of their starting weight. Statistical significance with respect to PBS is presented as $^{**}p < 0.01$ and $^{***}p < 0.001$. Statistical significance with respect to M2e/cGAMP MPs (60%) is presented as $\dagger p < 0.05$ and $\dagger\dagger p < 0.01$. Statistical significance with respect to solM2e + squalene is presented as $\ddagger p < 0.05$ and $\ddagger\ddagger\ddagger p < 0.001$ (n=14–15). Statistical analysis was performed using the Log-rank Mantel-Cox Test.

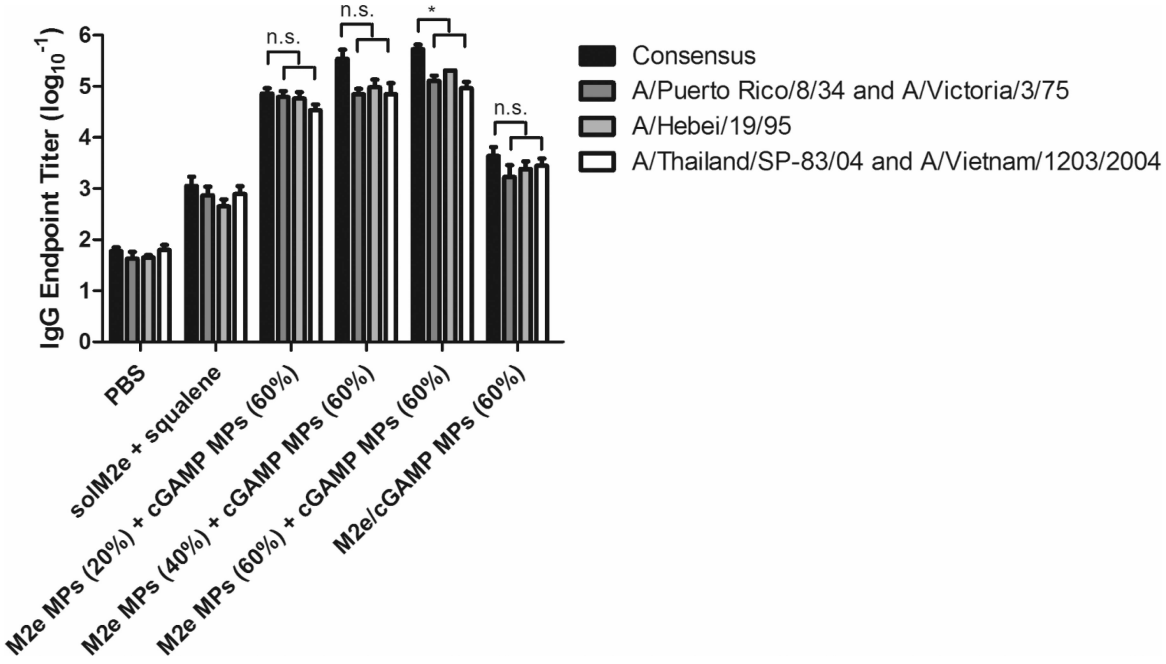

Figure 7.

Total IgG antibody titers against M2e sequences containing mismatch mutations to the consensus sequence. 1 mismatch (A/Puerto Rico/8/34 and A/Victoria/3/75), 2 mismatches (A/Hebei/19/95), and 3 mismatches (A/Thailand/SP-83/04 and A/Vietnam/1203/2004). Serum was collected on Day 28 after mice were vaccinated on Day 0 and 21 with phosphatebuffered saline (PBS), soluble M2e + MF59-like AddaVax (solM2e + squalene), M2e-loaded microparticles (M2e MPs (20, 40, or 60%)) + cGAMP-loaded microparticles (cGAMP MPs (60%)), or MPs containing both M2e and cGAMP (M2e/cGAMP MPs (60%)). All MPs were composed of acetalated dextran (Ace-DEX), and percentages indicate Ace-DEX MP relative cyclic acetal coverages. Pertinent groups received 10 μg M2e and 1 μg cGAMP. Statistical significance is presented as $*p < 0.05$, performed using a one-way ANOVA. Data are presented as mean ± standard error of the mean (n = 5).